Integrated Use of Geoelectrical Resistivity and Geochemical Analysis to Assess the Environmental Impact on Soil and Groundwater at Erbil Dumpsite, West of Erbil City - Iraqi Kurdistan Region

Sirwa Qader S. Gardi

Department of Geology, College of Science, University of Salahaddin, Erbil, Kurdistan Region - F.R. Iraq

***Abstract* - Water is one of the most important commodities which people and other creatures have exploited more than any other resources for their survival. Many parts of Erbil City and surroundings rely on groundwater reserves for drinking and other purposes. The study area lies within Erbil plain, some 10 km west of Erbil City. The study is based on the electrical resistivity method as a tool for assessing the environmental impact on soil and groundwater. Soil and water samples were collected close to Erbil dumpsite to assess the baseline data. 28 vertical electrical sounding points were taken by Schlumberger array along three geoelectrical sections. These sections revealed five zones of alternating clastic sediments with lateral changes which represent the Bai Hassan Formation. The average depth from the surface to the top of the aquifer is about 80 m. The geoelectrical sections revealed that the septic tank discharge valleys have been polluting the soil in two zones in the vicinity of the household septic discharge site. On the other hand, no adverse impact on groundwater quality is anticipated in the present project. The geophysical method utilized in this study is fast, efficient, and cost-effective in delineating the extent of the probable contamination zone(s).**

***Index Terms*—Resistivity, Geochemical, Groundwater, Soil, Dumpsite, Erbil.**

I. Introduction

During the past few years, the concern about the protection of the environment has largely increased due to the contaminants mainly with the anthropogenic origin and has affected and continue to threaten human resources, especially air quality, surface soil, and groundwater. The major problem facing the construction of new communities or development is the source of water. Kurdistan region, like many parts of the world, experiences problems in terms of shortage and degradation. Many factors affect water pollution such as industrial, agriculture, and the wastes and affluence released by human activity. With the dwindling price of oil and the most likelihood of future reliance on water for agriculture and industrial activities (agriculture, industry, and domestic), surface and groundwater sustainability and integrity are of paramount importance in Kurdistan region. In the cities of Kurdistan, the rate of abstraction in some areas exceeds recharge from rain and snow. Therefore, its protection is part of our responsibility of both governorate and public.

Iraqi Kurdistan Region has experienced an economic development, intense urbanization, and change in consumption patterns that have resulted in an increase of solid waste generation. As a result of population growth and construction expansion, there is a large increase in demand for water, building material, and cleared land, and consequently, in the amount of industrial and domestic waste production.

Groundwater resources have been under rapidly increasing stress in large parts of the world due to pollution. Pollution is primarily the result of irrigated agriculture, industrialization, and urbanization, which generates diverse wastes, with the attendant impact on the ecosystem and groundwater. With a rapid increase in population and growth of industrialization, groundwater quality is being increasingly threatened by the disposal of urban and industrial solid waste (Raju, *et al*., 2011; Singh, *et al*., 2015a).

Groundwater is a major source of water supply for domestic, agricultural, recreational, and industrial purposes in Erbil. Consequently, the adequacy of groundwater resources, both in quality and quantity, is essential for socioeconomic sustainability in the area. Groundwater resources are very important for public water supply. Many of the environmental problems are directly or indirectly related to the location of groundwater and its protection from contamination sources of various kinds.

The environment at which waste is disposed poses a major problem on groundwater. Solid wastes are produced every day in urban societies as a result of human activities and in

ARO-The Scientific Journal of Koya University
Volume V, No 2(2017), Article ID: ARO.10192, 13 pages
DOI: 10.14500/aro.10192
Received 14 January 2017; Accepted 02 October 2017
Regular research paper: Published 25 October 2017
Corresponding author's e-mail: sirwa.gardi@su.edu.krd

an attempt to dispose off these materials; man has carelessly polluted the environment (Badmus, *et al*., 2014). Pollution from solid wastes always begins with precipitates carrying the leachates into land surface and ends with the water reaching surface water or groundwater. During the vertical percolation process (with rainwater), the water leaches both organic and inorganic constituents from refuse. The leachates become part of the groundwater flow system immediately reaching the water table. The effects are generally the same, but their level may be changed according to the region (Gulmez, 1999).

Among all the surface geophysical techniques for shallow subsurface prospecting, electrical resistivity method is the most widely applied method for this purpose. Geoelectrical measurements are an important and integral component of geophysical investigations connected with environmental problems. Electrical resistivity survey methods have been widely used to solve engineering, archeology, environmental, and geological problems in the past decades (Adli, *et al*., 2010).

In groundwater studies, several geophysical methods have been deployed since late 1915, of which the electrical method has shown a wider approach and better applicability in groundwater science (Arshad, *et al*., 2007). Among those, electrical methods have been found very suitable for such studies, due to the conductive nature of most contaminants (Jegede, *et al*., 2012).

The study was assisted with the use of the geophysics, namely, the electrical resistivity method, as a tool to examine this impact, employed to characterize the contaminant through changing resistivity behavior pattern.

Vertical electrical sounding (VES) survey and hydrochemical analysis of the water and soil samples from the surrounding wells in the study area were adopted. These were used to determine the contamination spread both in lateral and vertical directions.

The aim of the study is to provide an understanding of the ground conditions (geological and hydrogeological information) pertaining to Erbil dumpsite. This study is hoped to enable a scientific approach to assess the environmental impacts on soil and groundwater based on the resistivity and geochemical methods of the subsurface layers.

II. Study area and description

The study area site lies within Erbil plain, about 10 km west of Erbil City, covering about 7 km^2 with Latitude 36° 11’ 40.60”N and Longitude 43° 53’ 05.10”E (Fig. 1), and located on a hill conjoined by two drainage valleys. The elevation of this site is about 435m above sea level.

The Erbil dumpsite operation life is since year 2001 (Municipal ministry) and currently receives all types of solid waste. Daily disposal is about 1000 ton of solid waste of varied types.

The location is generally used for any type of general household waste. The waste dumped at this site includes domestic waste, for example, kitchen waste, food leftovers, paper, newspaper, metal and glass cans, packaging, plastic, glass, cartoon, wood, metals, ceramics, leather, cloths, and batteries (Fig. 2). These wastes can spontaneously ignite and produce noxious smoke smell and which varies according to waste composition with greater risk to the operating management staff. Construction and demolition wastes, which consist of sand, bricks, and concrete block, are also dumped. Dumping activities started from the top of the site by merely toppling the waste over the edge.

Some components of the waste are very hazardous or toxic such as liquid solvents seen along one of the valleys, north of the Erbil dumpsite ridge. Furthermore, it was observed that black water from household septic tanks was also discharged nearby the site.

With an increasing population in Erbil City, as the capital of the Iraqi Kurdistan Region, and changing production and consumption patterns in the past few years, the levels of degrading waste are increasing at alarming rates.

Existing waste disposal sites are rapidly filling up and with the ever-increasing costs for disposal of waste; it is becoming very difficult and expensive to dispose of food waste which is the main waste in the Erbil dumpsite. Therefore, any sector that generates food waste is facing a potentially huge disposal problem, particularly those establishments catering on a large scale, such as hospitals, schools, universities, Ministry of Defense sites, prisons, hotels, restaurants, and even shopping centers and parks, in addition to household food waste. The wastes in the Erbil dumpsite are decomposing continually, and a sludge of decomposed soup known as leachate will develop.

III. Geology and hydrogeology of the study area

The study area lies within the Chemchamal-Butma subzone of the foothill zone, which is the central unit of the Unstable Shelf. Butma-Chemchemal subzone, however, has very conspicuous long and deep synclines with thick Pliocene molasses dominated by a conglomerate, and the strata are neccessarily horizontal (Jassim and Goff, 2006). Erbil plain is considered to be among these plains as a broad syncline between two main anticlinal structures, Pirmam from the east and Khurmala-Avana from the west (Hassan, 1998). The inner parts of the synclines contain quaternary deposits, referred to here as the polygenetic synclinal fill. The geological formations in the study area are described from the older to younger rock units as follows: Mukdadiya Formation (Pliocene): It comprises of fining upward cycles of gravely sandstone, sandstone, and red mudstone (Jassim and Goff, 2006) and Bai Hassan Formation (Pliocene): It consists of molasses sediments represented by alternation of clay stones and conglomerates with some sandstones and siltstones, variations from one of the main constituents to the other, both laterally and vertically is very common (Hassan, 1998). The major part of the study area is covered by this formation (Fig. 3). No accurate information is present about the thickness of this formation and quaternary deposits (Pleistocene- Holocene): Quaternary sedimentary veneer of polygenetic origin covers large areas in the synclines of the foothill zone. These synclines often have

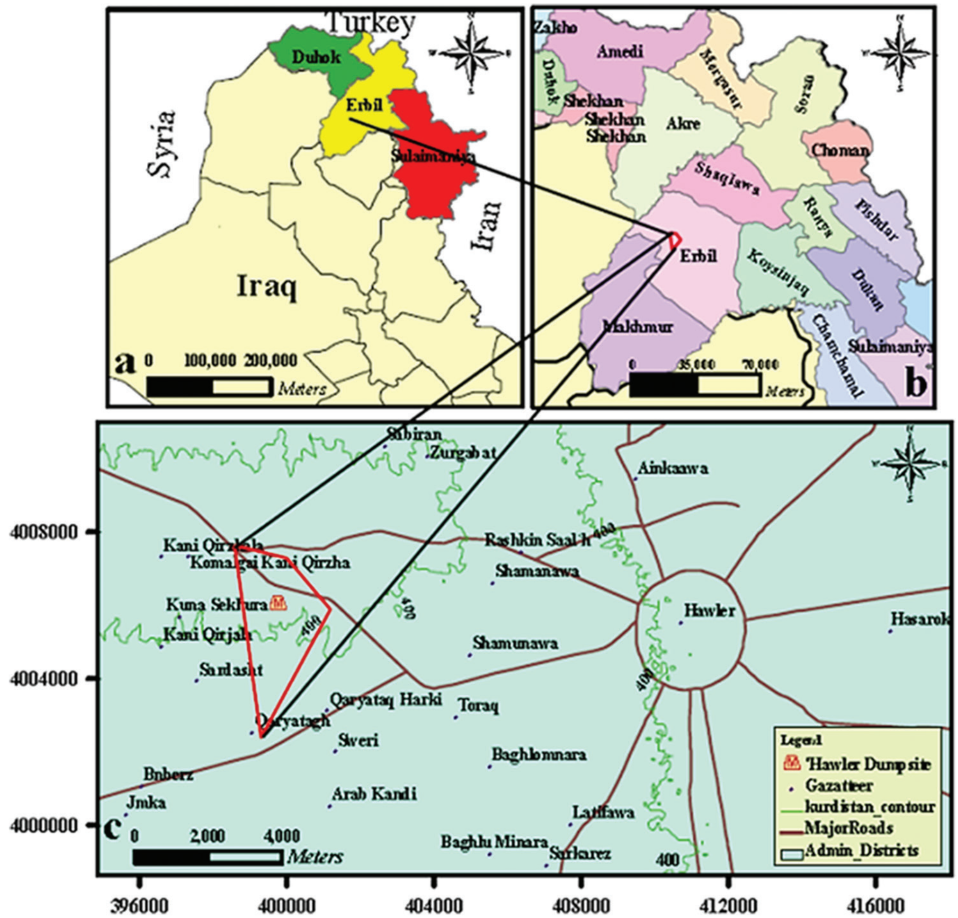

Fig. 1 (a) Iraq, location of Erbil province is indicated, (b) Kurdistan Region of Iraq, and (c) Erbil City, location of the study area is indicated (red line)

Fig. 2 Variety types of solid waste in the Erbil dumpsite

a central river system that cuts across or flows parallel to their axes, and the sediments filling the synclines consist mainly of a mixture of gravel and clay (Jassim and Goff, 2006).

Erbil hydrogeological basin is bounded by Greater Zab from north and Lesser Zab to the south. Erbil basin is a wide depression located between southern limb of Pirmam anticline and Dibaga hill zone (Zurgah Zraw Zurg) which gives a semicircular shape to Erbil basin (Majeed and Ahmad, 2002). The Pliocene formations, and especially the Bai Hassan, is considered as a major aquifer in the Erbil basin, and it is a continental deposit of gravel, conglomerate, sand, and clay. Depth to groundwater varies in short distances due to variable topography. In general, the Erbil Basin is divided into three sub-basins, which include the Northern (Kapran) sub-basin, the Central sub-basin, and the Southern (Bashtapa) sub-basin (Habib, *et al*., 1990). The study area is located in the central sub-basin. This sub-basin has an area of 1400 km^2. The formations in this sub-basin are the Mukdadiya and Bi Hassan Bakhtiary Formations and alluvium. The Bi Hassan formation consists of gravel, sand, clay, and conglomerate strata. However, in some of the deep wells in the Mukdadiya, formation consists of thin beds of gravel, sand, or conglomerate. The materials of alluvium aquifers are the same as Bi Hassan Bakhtiari Formation, with the exception that they contain silt in between the other layers instead of multiple clay layers (Dizayee, 2014). According to Hassan (1998), the groundwater table depth ranges between 30 and 50 m in Erbil City, and according to Al-Ansari, *et al*. (1981), the water table is usually 50 m deep. Hassan (1998), during his study, noticed that the groundwater moves from east to west side of the Erbil city, so it flows in the same direction as regional groundwater flows.

 http://dx.doi.org/10.14500/aro.10192

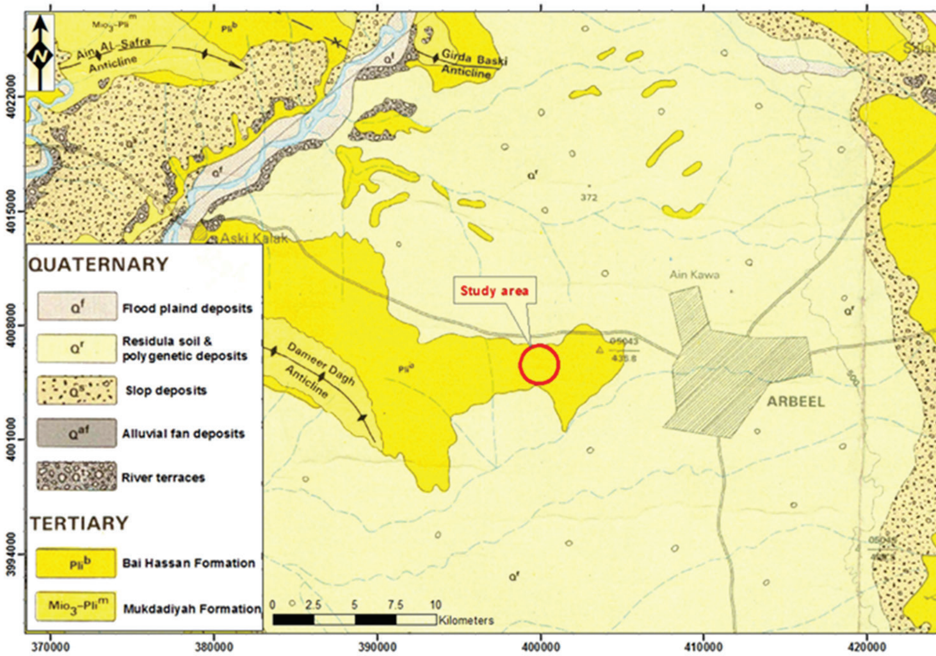

Fig. 3 Geological map showing the study area (After Sissakian, 1997)

IV. Methods of investigation

A. Geophysical Technique

Resistivity measurements with electrical resistivity method are one of the simplest methods to be used in geophysics. Electrical method is used to determine the subsurface resistivity distribution by making suitable measurements on the surface. VES is used in this study to measure variation in resistivity with depth. VES uses direct current (DC) injected into the ground surface to investigate the subsurface electrical resistivity (Vladimir, *et al*., 2006). DC resistivity methods use artificial sources of current to produce an electrical potential field in the ground. A current is introduced into the ground through point electrodes (A and B) and the potential field is measured using two other electrodes (the potential electrodes M and N) (Fig. 4). As the potential between M and N, the current introduced through A and B, and the electrode configuration is known, the resistivity of the ground can be determined; this is referred to as the "apparent resistivity" (Knodel, *et al*., 2007).

The resistivity survey was completed with twenty-eight VES points along three traverses A-A¯, B-B¯, and C-C¯ (Fig. 5). An ABEM Terrameter SAS 300B was utilized to acquire the VES data. The Schlumberger array was used with a maximum current electrode spacing (AB) ranging from 600 to 800 m (AB/2 ranging from 300 to 400 m). Schlumberger field array is usually used because it has proven effective for groundwater exploration (Edwards, 1977; Zohdy, *et al*., 1984). The Schlumberger configuration is symmetric and collinear and uses four electrodes (Evanston, 1979). The spacing between the potential electrodes is fixed and is less than the separation between the current electrodes which is progressively increased during the survey (Oghenekohwo, 2008). In a traditional Schlumberger or Wenner electrical sounding, the transmitting A and B electrodes are successively moved away from each other at each new reading to increase the depth of investigation (Bernard, 2003). The measured resistance values were converted into apparent resistivity (ρa) by multiplying with a geometric factor (K), such that

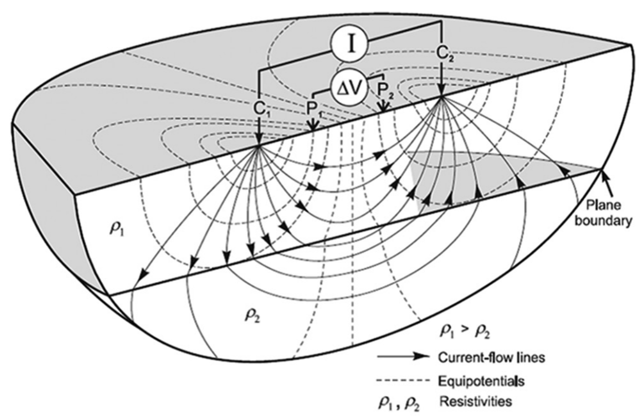

Fig. 4 Principle of resistivity measurement with four-electrode array (Knodel, *et al*., 2007). Where C1 = A, C2 = B, P1 = M, and P2 = N

$$\rho a = \frac{\pi\left[(AB/2)^2 - (MN/2)^2\right]}{MN} \quad (1)$$

$$\rho a = K.R \quad (2)$$

The length of each traverse is 700 m, 800 m, and 900 m, respectively. The direction of the first and second traverses is parallel which are directed from NW to SE and the last traverse is directed from NE to SW. Location fixing and topographical heightening of the sample points and wells were achieved by means of twelve channel global positioning system (GPS) set - the “GARMIN GPS 12.” The resistivitimeter measures the apparent resistance directly. These measurements are then converted to apparent resistivity values by scaling them by a geometrical factor that depends on the type of array as well as the spacing between the electrodes. The last VES point was taken near the Tashyapi well to calibrate the instrument. The sounding spacing was about 100 m, and four of these VES points have been conducted near to existing wells for correlation purposes and obtaining the lithological and hydrogeological information (Fig. 4). The key to the success of any geophysical survey is the calibration of the geophysical data with hydrogeological and geological ground true information (Lashkaripour and Nakhaei, 2005). The spreading of electrodes is parallel to the general structure direction around the study area (NW-SE), though the beds in the study area are distributed subhorizontally because they are distributed in the broad polygenetic deposits.

B. Geochemical Methods

Soil and water samples were collected nearby the Erbil dumpsite to assess the baseline data.

Soil sample analysis

Soil samples were collected from different locations at about 25 cm depth within the activity area including three samples (Fig. 6). The pH of soil samples was measured by pH meter equipment and electrical conductivity (EC) by EC equipment in the Chemistry Department laboratory in Science College-Salahaddin University. The soil class is clay loam in first two samples and silty clay loam in sample three. The pH of soil is strongly alkaline based on the classification of Al-Agidi (1989) (Table I).

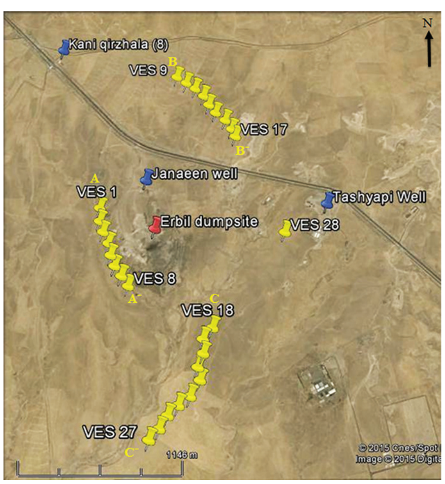

Fig. 5 Map showing the vertical electrical sounding points and calibration wells at the study area

Water sample analysis

Furthermore, water samples were collected from three water wells at different locations above and behind the Erbil dumpsite (Fig. 6). Major cations and anions were analyzed to determine the level of their contamination. The result obtained was compared with the International standard for drinking water after “WHO” to determine the level of contamination (If any). The pH measurements show that all water samples are of basic type. The chemical composition of the water wells compared with the WHO (2003) is given in (Table II). All water analyzed samples are suitable for drinking and irrigation.

Analyzed in the laboratory of Directorate of Water Quality Control Department in Erbil.

V. Geophysical data processing

There are many computer programs to compute and process the resistivity field data. Inspite of various uses of different programs, the final decision or assessment of inversion results is dependent on the user (geophysicist). Several computer programs are available for the inversion, allowing data processing, as well as editing of data sets and sounding array parameters or shifting of overlapping segment to produce continuous sounding curves. The inversion method is equivalent to matching automatically the observed and theoretical curves (Lowrie, 1997). The interpretation as determined by the program is mathematically correct but may not necessarily correspond to reality (Compbell and Horton, 2000). The interpretation of each VES curve was carried out by the use of automated interpretation computer program IPI2WIN (2001) (Fig. 7).

The IPI2WIN program is designed for VES and/or induced polarization data curves or 1D interpreting along a single profile, obtained with any of a variety of the most

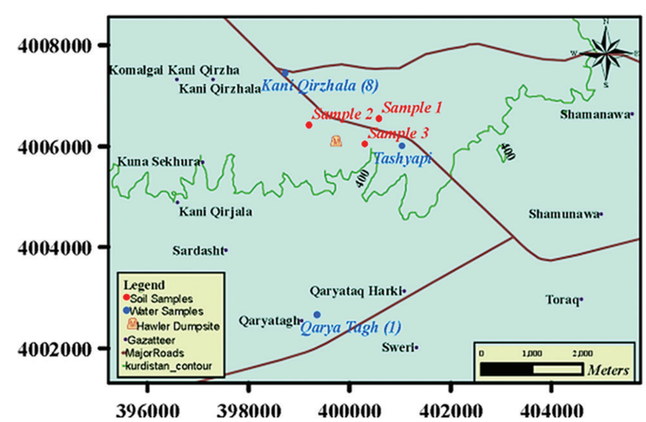

Fig. 6 Map showing water and soil samples locations

Table I Soil Sample Analysis

Sample No.	Class (Mirsal, 2008)	Texture (grain size) (Al-agidi, 1989)	Color (Munsell Book of Color, 1975)	Moisture content%	pH	EC (mS/cm)
1	Clay loam	Moderately to medium	Very dark brown	16.96	8.7	8.25
2	Clay loam	Moderately to medium	Dark-yellowish brown	13.25	8.7	13
3	Silty clay loam	Moderately to medium	Dark-yellowish brown	15.61	8.6	9.95

http://dx.doi.org/10.14500/aro.10192

TABLE II WATER SAMPLE ANALYSIS (MG/L)

Parameters	Tashyapi	Kani Qirzhala	QaryaTagh	WHO (2003)
Turbidity (NTU)	0.6	0.4	0.4	5
pH	7.6	7.4	7.1	8
EC (mmho/cm)	1062	703	516	1530
T.D.S.	680	450	330	1000
Hardness (as mg $(caco_3)$/l)	340	232	286	500
Ca	44	47	49	200
Mg	39	43	38	150
Na	16	9	12	200
K	0.51	0.65	0.59	3
HCO_3	20	31	37	200
SO_4	47	41	44	250
Cl	29	21	11	250
NO_3	5	8	8	50

popular arrays used in the electrical prospecting. It is presumed that a user is an experienced interpreter willing to solve the geological problem posed as well as to fit the sounding curves (Geoscan-M Ltd., 2001). In this program, the half distance between current electrodes spacing (AB/2), potential electrode spacing (MN), and apparent resistivity measurements is given to obtain resistivity curves.

VI. GEOPHYSICAL INTERPRETATION

The field results of the study are presented in both qualitative (curve shapes) and quantitative interpretations. Vertical sounding field curves can interpret qualitatively using simple curve shapes, semi-quantitatively with graphical

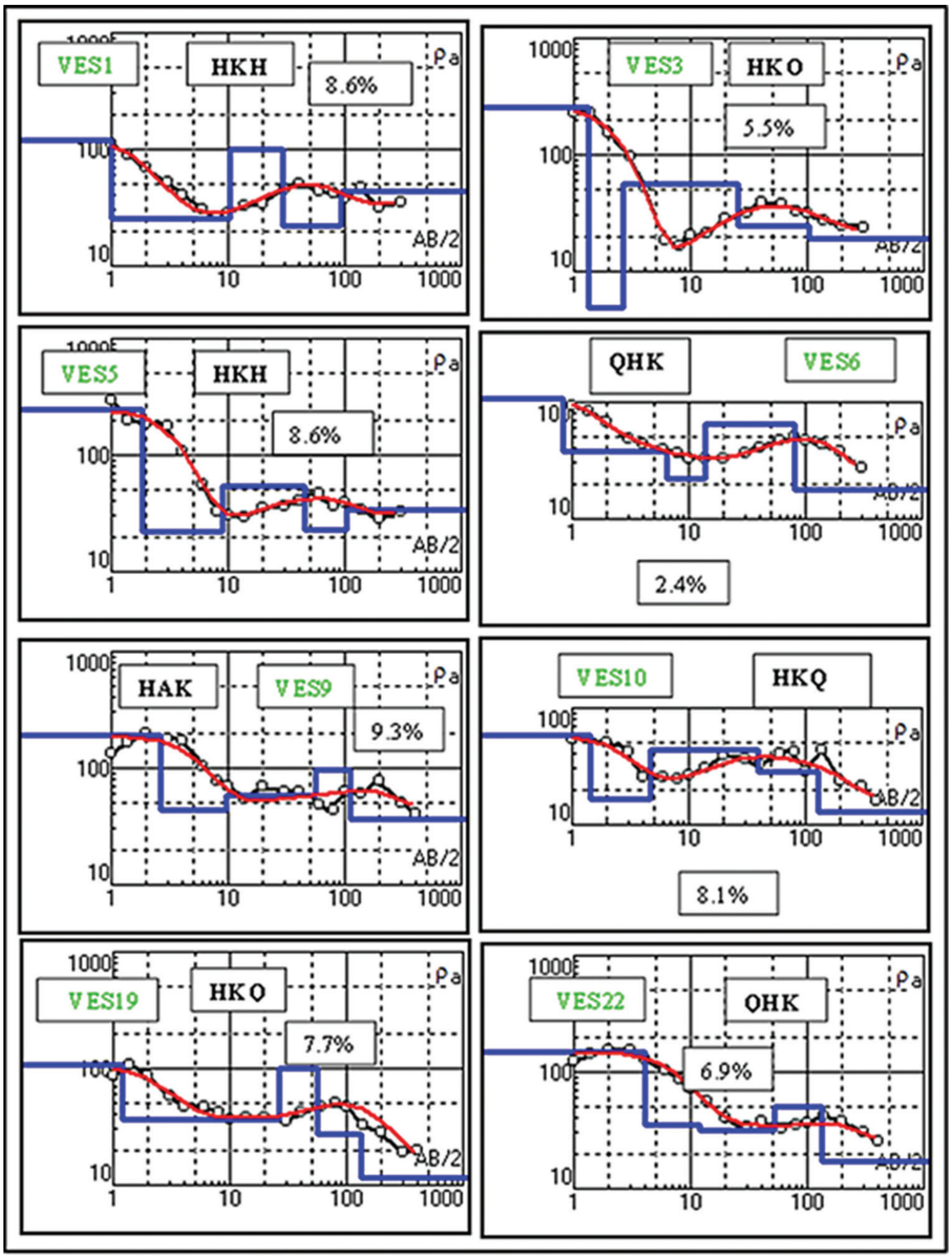

Fig. 7 Some examples of field curves along traverses A-A¯, B-B¯, and C-C¯ interpreted by IPI2WIN (2001). X- axis: Resistivity (Ω.m), Y- axis: Spacing (AB/2) (m). Where VES9: VES point, HKQ: Curve type and 8.1% error percentages

model curves, or quantitatively with computer modeling (Reynolds, 2011). In the qualitative interpretation, the shape of the field curve is observed to get an idea qualitatively about the number of layers and the resistivity of layers. The results of this method of interpretation involved isoapparent electrical resistivity maps and geoelectrical pseudosections. In the quantitative method geoelectrical parameter, that is, true resistivity and layer thickness are obtained. The main objective of the quantitative interpretation of VES curve is to obtain the geoelectrical parameters and geoelectric section. A geoelectric layer is called by its fundamental characters, resistivity "ρ" and thickness "h." It is hoped that the results of this study could also be used to determine the groundwater potentials of the study area.

A. Qualitative Interpretation

The first stage of any interpretation of apparent resistivity sounding curves is to note the curve shape. A first appraisal of an area hydrogeologically can often be obtained by merely looking at the shapes of the field curves (type curves) and the ranges of apparent resistivity values. The shapes of curves are dependent on the thickness, resistivity, and outer electrode spacing of layers. Due to the distinctive characteristics feature in the field of the apparent resistivity curves, the VES stations show various types of field curves. These types of curves were defined in terms of the number of geoelectrical layers and their respective resistivity relationships.

Twenty-eight VES points were taken. We can group these VES points into ten groups, which all VES points are composed of five layers (Fig. 7). They reflect that the study area is composed of various types of sediments (heterogeneous). Among these types of curves, most of them are layer resistivities decreasing with depth. Such layers prove the presence of a low resistivity layer at the bottom of the section. By collecting the prior information from the water wells near the study area and geological information which have been conducted around and nearby the study area, we can conclude that the study area is composed of clastic materials.

B. Quantitative Interpretation

The mathematical analysis for quantitative interpretation of resistivity results is most highly developed for the vertical sounding technique (Telford, *et al.*, 1990). The quantitative treatment of the VES provided geoelectrical information characterized by the values of true resistivity and thickness. These geoelectrical parameters define the geoelectrical model. The latter will provide resistivity models whose layer boundaries are boundaries of geoelectrical layers but not necessarily of lithological layers (Knodel, *et al.*, 2007). The inversion of the field data was done using the IPI2WIN (2001) program (Table III). The results of inverse modeling are very close to the manual interpretation. The IPI2WIN data were used for interpretation and making geoelectrical sections. The geoelectrical model was determined as a function of the calibration with the data from wells and the resistivity contrast between high and low values. Overall, the results confirm that topographical variations of the study area can have a significant impact on measured resistivity data values and show that the significance of the distortions will vary according to the details of the topography and survey type. The resulted data (true resistivity and thickness) can be interpreted quantitatively through the geoelectrical sections.

VII. Geoelectrical sections

Geoelectrical sections can be constructed by linking a number of VES points which are located along one straight line. They will show the vertical and lateral distribution of resistivities of subsurface layers. Each layer in geoelectrical sections is characterized by its thickness and ranges of true resistivity and will give an idea of the kind of rock present in the subsurface, and hence, a model of the subsurface can be prepared (Oghenekohwo, 2008).

The resulting geoelectric models are used to produce three geoelectrical sections: Traverses A-A^{-}, B-B^{-}, and C-C^{-}. Each section has its characteristics of true resistivity and depth, and its lithology can be interpreted in detail in each geoelectrical section.

A. Geoelectrical Section Along Traverse A-A^{-}

This section shows the presence of five subsurface geoelectrical zones (Fig. 8). A first (Z1) continuous thin surface nearly horizontal zone is represented by topsoil with resistivity ranging from 47 to 421 Ω.m. These variations in

Table III The True Resistivity, Thickness, and Curve Types of Each Layer Which was Interpreted by IPI2WIN (2001) Program

VES No.	True resistivity (Ω.m)					Thickness (m)			
	ρ1	ρ2	ρ3	ρ4	ρ5	h1	h2	h3	h4
VES1	119.0	25.6	99.2	21.7	43.7	0.99	9.36	18.7	65.7
VES 2	47.1	3.82	322.0	26.1	17.6	1.06	1.59	6.07	66.4
VES 3	253.0	3.16	56.0	24.3	18.8	1.35	1.29	23	76.7
VES 4	421.0	35.7	50.3	23.8	17.7	1.22	18.4	41.1	40.8
VES 5	247.0	21.8	55.1	22.8	33.6	1.84	6.98	36.0	57.5
VES 6	108.0	37.7	21.7	64.6	17.8	0.83	5.56	7.52	66.2
VES 7	252.0	48.0	28.5	49.2	22.2	0.26	2.23	17.6	62.9
VES 8	274.0	38.7	25.5	69.5	16.3	1.3	9.86	21.2	50.7
VES 9	190.0	43.7	58.2	95.5	36.1	2.63	7.07	47.2	54.5
VES 10	58	16.8	43.5	28.5	12.8	1.43	3.32	34.3	87.6
VES 11	51.25	26.55	46.41	26.99	14.94	1.24	4.31	41.51	95.06
VES 12	98.0	27.90	37.70	22.50	11.70	1.77	3.52	55.4	66.0
VES 13	111.0	25.30	78.60	28.70	12.90	1.58	12.8	39.40	73.80
VES 14	139.0	28.4	81.1	17.0	10.20	2.45	8.78	46.1	58.5
VES 15	131.0	37.80	20.40	31.90	61.0	1.32	6.44	22.9	100.0
VES 16	106.0	10.70	59.70	11.10	26.70	1.71	3.43	19.90	101.0
VES 17	77.5	165	58.7	28.4	21.0	1.02	0.94	58.1	69.0
VES 18	112.0	27.5	161.0	69.0	15.30	6.19	33.4	36.60	54.90
VES 19	106.0	36.10	98.50	26.90	11.40	1.2	25.4	29.90	76.60
VES 20	117.0	49.90	28.80	22.20	33.40	2.87	20.2	30.0	77.0
VES 21	192.0	1.96	46.20	29.50	10.20	4.43	4.38	33.90	88.30
VES 22	146.0	35.80	31.60	49.90	17.20	4.08	8.05	40.50	80.70
VES 23	58.8	99.20	34.20	28.20	34.40	0.83	8.88	49.0	72.30
VES 24	41.9	79.5	21.10	25.20	46.80	0.90	20.40	22.0	88.0
VES 25	27.80	42.60	67.90	30.0	37.20	2.22	8.45	24.90	96.20
VES 26	48.6	93.10	20.30	15.10	35.90	1.92	9.54	29.60	89.8
VES 27	88.70	40.40	22.80	33.60	13.50	0.78	11.8	24.30	94.40
VES 28	192.0	42.10	17.60	35.0	16.40	2.55	12.40	22.40	94.70

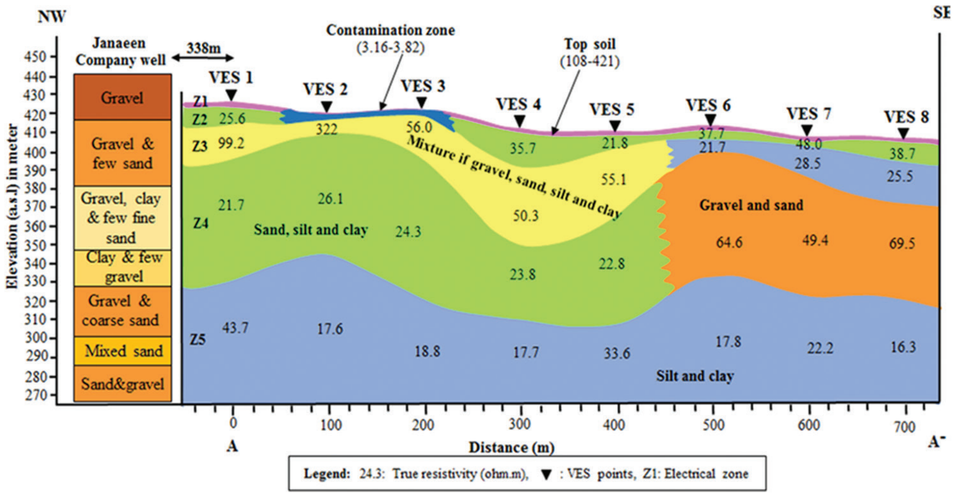

Fig. 8 Geoelectrical section along traverse A-A¯

resistivity value occur due to various types of sediments, fine and medium, to coarse grained material of sand and gravel with high ratio of relatively coarse gravel. The thickness varies from 0.25 to 1.85 m. The second geoelectrical zone (Z2) has resistivity ranging from 3.0 to 48.0 Ω.m and thickness ranging from 1.0 to 18.0 m. The resistivity is diagnostic of fine-grained sediments such as sand, silt, and clay. This geoelectrical section is in a contaminated area and shows a low resistivity ranging from 3.0 to 4.0 Ω.m under VES points VES2 and VES3 compared to those of the uncontaminated layer outside the disposal site and thickness of 1.0-1.5 m. It may be contaminated with the septic tanks discharge. Furthermore, the curve type is of HKQ type which shows the low resistivity value in this layer. The resistivity of the third zone (Z3) has values from 50.0 to 322.0 Ω.m and thickness ranging from 6.0 to 41.0.5 m. This horizon is composed of mixture gravel, sand, silt, and clay. The resistivity value under VES point VES2 is too high (322 Ω.m), due to the increase of the ratio of gravel toward the NW compared to other continuous VES points which are composed of mixture of gravel, sand, silt, and clay with lateral change to silt and clay (21.0-28.5 Ω.m) and thickness ranging from 7.0 to 21.0 m under VES points 6, 7, and 8. The fourth geoelectrical zone (Z4) of this geoelectrical section has resistivity ranging from 21.0 to 26.0 Ω.m and thickness from 40.0 to 76.0 m. This layer consists of sand, silt, and clay with lateral changes to a mixture of gravel, sand, silt, and clay (49.0-70 Ω.m) and thickness ranging from 50.0 to 66.0 m toward the Southeast direction of the study area. The fifth geoelectrical zone (Z5) has resistivity value ranging from 16.0 to 43.0 Ω.m. The thickness of this layer is not defined since it is the last layer. This layer consists of fine sediments such as silt and clay saturated with groundwater.

B. Geoelectrical Section Along Traverse B-B¯

This section shows the presence of five subsurface geoelectrical zones, which nearly has the same lithology, with difference of the layer thicknesses (Fig. 9): A first (Z1) is a continuous thin surface nearly horizontal zone is represented by topsoil with resistivity ranging from 51.0 to 191.0 Ω.m. These variations in resistivity value occur due to various types of sediments, fine and medium, to coarse-grained sand and gravel with variable size. The thickness varies from 0.5 to 2.5 m. The second geoelectrical zone (Z2) has resistivity ranging from 11.0 to 40.0 Ω.m and thickness ranging from 3.0 to 13.0 m. This horizon is not found under VES point 17. The resistivity is diagnostic of fine-grained sediments such as sand, silt, and clay. Furthermore, the curve type of this traverse shows the low resistivity value of HKQ type. The resistivity of the third zone (Z3) ranges from 37.0 to 81.8 Ω.m and thickness ranges from 20.0 to 58.0 m and becomes thinner at about 20.0-23.0 m under VES points 15 and 16. This horizon is composed of a mixture of gravel, sand, silt, and clay with high ratio of gravel under VES points 13 and 14. This horizon contains lens representing silt and clay (20.4 Ω.m) of about 23 m under VES point 15. The fourth geoelectrical zone (Z4) in this geoelectrical section has resistivity ranging from 11.0 to 32.0 Ω.m and thickness from 54.5 to 101.0 m. This horizon consists of sand, silt, and clay while the VES point 9 has high resistivity value (95.5 Ω.m) with about 69.0 m which may be interpreted due to increasing the ratio of gravel and sand toward the Northwest direction of the study area. The fifth geoelectrical zone (Z5) which represents an aquifer of groundwater has resistivity value ranging from 10.0 to 36.0 Ω.m (the curve types of this traverse are of HKQ and KQQ type) lateral lithological variations to coarser material with resistivity (61.0 Ω.m) under VES point 15 (as shown in curve type QHA). The thickness of this horizon is not defined since it is the last horizon. This horizon consists of fine sediment such as silt and clay with lateral lithological variations to coarser material such as a mixture of gravel, sand, silt, and clay.

C. Geoelectrical Section Along Traverse C-C¯

Furthermore, this section shows the presence of five subsurface geoelectrical zones. Thickness and lithology of the layers are as follows (Fig. 10): A first (Z1) uncontinuous thin surface nearly horizontal zone occurs at along traverse

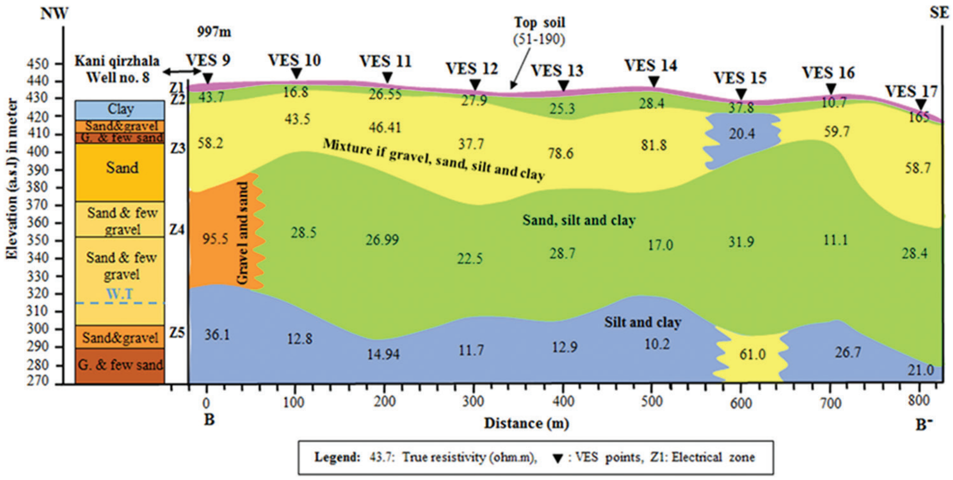

Fig. 9 Geoelectrical section along traverse B-B¯

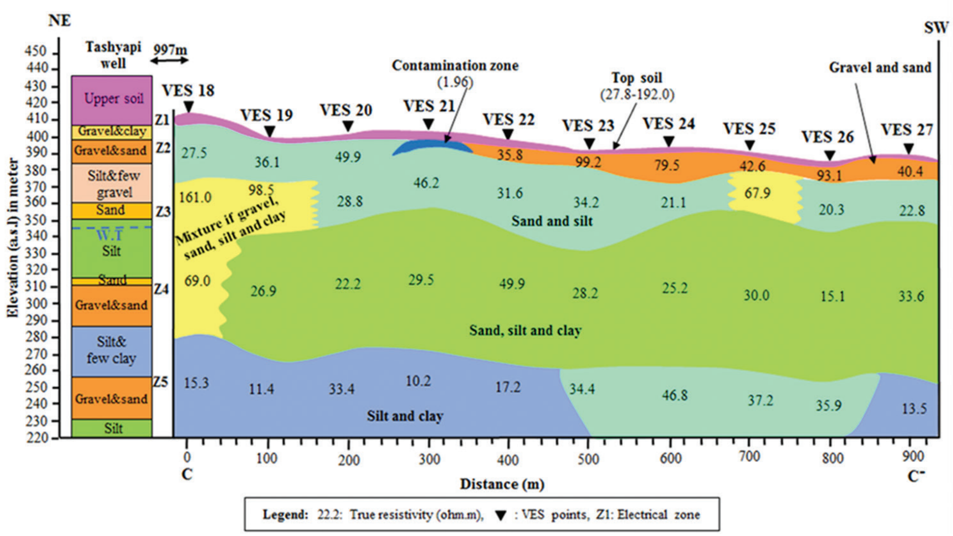

Fig. 10 Geoelectrical section along traverse C-C¯

represented by topsoil with resistivity ranging from 28.0 to 192.0 Ω.m. These variations in resistivity value occur due to various types of materials, fine- and medium-grained material of sand and gravel. The thickness varies from 0.8 to 6.0 m. The second geoelectrical zone (Z2) has a resistivity ranging from 27.5 to 99.2 Ω.m and a thickness ranging from 8.0 to 33.0 m. This horizon is composed of a mixture of gravel, sand, silt, and clay. In this section, a lens was shown within this horizon having a resistivity of about 2.0 Ω.m with a thickness about 4.5 m beneath VES point 21 (as shown in curve types HKQ). This lens may be representing the contaminated area because it is susceptible to pollution by septic tank discharges. The third geoelectrical zone (Z3) in this section has a resistivity ranging from 20.0 to 46.0 Ω.m and a thickness ranging from 22.0 to 49.0 m. This horizon is composed of sand and silt with lateral changes to a mixture of gravel, sand, silt, and clay with resistivities ranging from 67.0 to 161.0 Ω.m and a thickness ranging from 25.0 to 36.0 m under VES points 18, 19, and 25. Al-Naqib (1959) according to a geological study on the Bai Hassan formation mentioned that it is composed of an alternation of conglomerate, clay, and sand as large lenses and lateral rapid changes. Furthermore, the fourth geoelectrical zone (Z4) is present, and the same lithology (aquifer) was observed with relatively higher resistivity than other two geoelectrical sections, ranging from 15.0 to 50.0 Ω.m except under VES point 18 [69.0 Ω.m] due to changes in the lithology to mixture of gravel, sand, silt, and clay. This horizon consists of sand, silt, and clay which represent an aquifer of good quality groundwater. The thickness of this aquifer ranges from 55.0 to 96.0 m. The fifth geoelectrical zone (Z5) has resistivity value ranging from 10.0 to 33.0 Ω.m which is composed of fine sediments such as silt and clay with lateral variation to sand and silt (34.0-47.0 Ω.m). The thickness of this horizon is not defined since it is the last horizon.

VIII. Hydrogeological Assessment

The results of the three geoelectrical sections in the study area show successions with variable lithology and thickness.

 http://dx.doi.org/10.14500/aro.10192

This lithology reflects the Bai Hassan formation as given by Buday (1980) as he mentioned that the formation consists of molasses sediments represented by the alternation of clays and conglomerate with some sandstones and siltstones. The horizon that is composed of silt and clay and sand and silt is representing an aquifer in the study area in both tarverses A-A¯ and B-B¯, whereas in traverse C-C¯, the sand, silt, and clay horizon represent an aquifer. According to Stevanovic and Iurkiewicz (2009), it consists almost entirely of terrigenous clastics from silt size to boulder conglomerates (eroded and transported from the Zagros Mountains). The successive repetition of the fine-, medium-, and coarse-grained textures and the variation in permeability from one site to another within the same aquifer horizon are typical characteristics of this aquifer. Ghaib (2003) and Ghaib and Aziz (2002) during their studies on parts of Erbil City concluded that the resistivity of the saturated rock unit (mixture of clay, silt, sand, and gravel) ranges from 15 to 45 Ω.m. It is in a good agreement with the resistivity of the aquifer unit in the geoelectrical sections ranging from 10 to 69 Ω.m. The depth to the top of the aquifer from the surface is approximately ranging from 35.0 to 129.0m (Table IV). From the ground surface as the deep water, table has been detected ranging from 55 to 94 m by Ghaib and Aziz (2002) in parts of Erbil city. There is a deeper water table which was drilled; it may be due to the drought condition which has been facing our region since that time.

Table IV Represent the Depth, Resistivity, and Elevation of the Top Surface of Aquifer

VES NO.	Elevation a.s.l (m)	Depth to the top of aquifer (m)	Elevation of top surface of aquifer a.s.l (m)	Resistivity of aquifer (Ω.m)
VES1	426	94.7	421.3	43.7
VES 2	420	75.1	344.9	17.6
VES 3	423	102.0	321.0	18.8
VES4	413	102.0	311.0	17.7
VES5	411	102.0	309.0	33.6
VES6	414	80.1	333.9	17.8
VES7	407	83.0	324.0	22.2
VES8	407	83.1	323.9	16.3
VES9	438	111.0	327.0	36.1
VES10	440	127.0	313.0	12.8
VES11	438	127.6	310.4	14.9
VES12	434	127.0	307.0	11.7
VES13	434	128.0	306.0	12.9
VES14	437	116.0	321.0	10.2
VES15	429	131.0	298.0	61.0
VES16	432	126.0	306.0	26.7
VES17	423	129.0	294.0	21.0
VES18	414	76.2	337.8	69.0
VES19	400	56.5	343.5	26.9
VES20	402	53.1	348.9	22.2
VES21	403	42.7	360.3	29.5
VES22	398	52.6	345.4	49.9
VES23	392	58.7	333.3	28.2
VES24	393	43.3	349.7	25.2
VES25	391	35.6	355.4	30.0
VES26	385	41.1	343.9	15.1
VES27	388	36.9	351.1	33.6

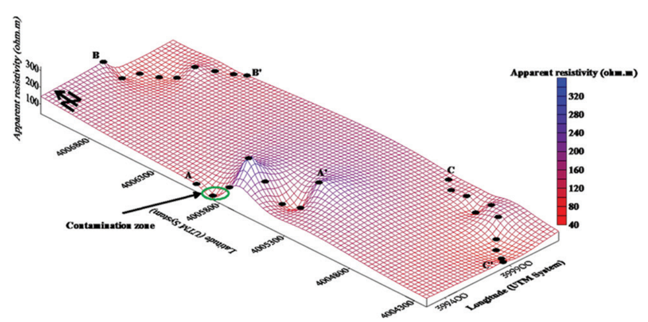

Fig. 11 Three-dimensional illustration of apparent resistivity values for half distance current electrode (1.4 m) (the origin of the block diagram coincides at each of the electrical sounding points [VES1-VES27])

IX. Environmental assessment of resistivity study (detection of contamination zone)

From the results of geoelectrical resistivity, the contaminated area was indicated by its low resistivity value if compared with surrounding area. The contamination zone is detected in the geoelectrical section along traverse A-A¯ under VES points 2 and 3 in the contaminated area by septic tanks. The thickness of this zone is about 1.0-1.5 m (Figs. 11-13) which shows the impact of septic tanks to the near subsurface layers. In this study, we choose the spacing that shows the effect of the contamination which is related to the environment. It can flow by infiltration from the surface to the downward due to the high porosity and permeability of the lithology. If this process is continued, it may be in contact with groundwater surface and finally contaminate the groundwater. The depth that is subjected to contamination from the surface is about (1.0-18.0 m). The contamination zone at the geoelectrical section along traverse C-C¯ was detected also by its vicinity to the septic tank discharging valley (Fig. 14). The thickness of this zone is about 4.0 m under VES point 21. The water is from the Bakhtiari aquifer, and recent deposits are generally also of good quality, with the exception of the waters from shallow wells, located near cities and villages, which are often contaminated, mainly as a result of the free seepage of sewage water (Stevanovic and Iurkiewicz, 2009). The contamination zone is not detected at the geoelectrical section along traverse B-B¯ because it is far away from the dumpsite and septic tank impacts.

X. Results and discussion

Areas near waste disposal sites have greater possibility of groundwater and soil contamination because of the potential pollution source of leachate and septic tanks discharge area originating from the nearby site. Such contamination of groundwater resource poses a substantial risk to local resource user and to the natural environment.

Erbil dumpsite, agricultural, and industrial activities (Fig. 15) have been identified as the main pollution sources to groundwater and soil in the study area. The main flows of heavy metals to the environment are from industrial and municipal wastes, both of which contained a variety of toxic

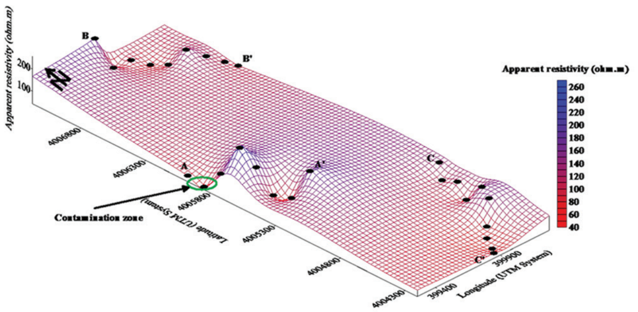

Fig. 12 Three-dimensional illustration of apparent resistivity values for half distance current electrode (2 m) (the origin of the block diagram coincides at each of the electrical sounding points [VES1-VES27])

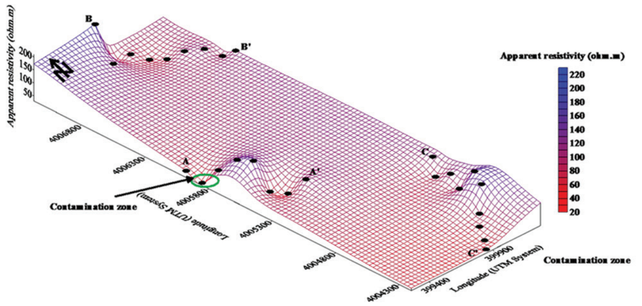

Fig. 13 Three-dimensional illustration of apparent resistivity values for half distance current electrode (3 m) (the origin of the block diagram coincides at each of the electrical sounding points [VES1-VES27])

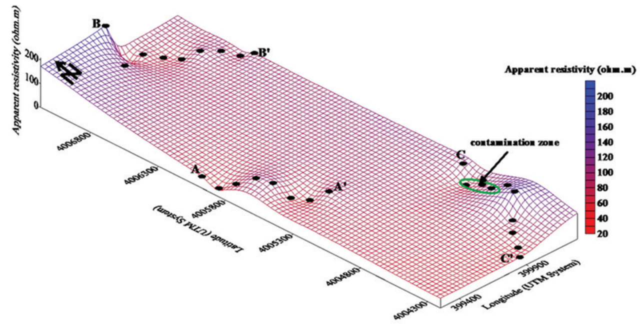

Fig. 14 Three-dimensional illustration of apparent resistivity values for half distance current electrode (4 m) (the origin of the block diagram coincides at each of the electrical sounding points [VES1-VES27])

Fig. 15 Industrial wastes in the study area (agricultural plots)

heavy metals (Chuangcham, *et al*., 2008). This problem is important, especially when industrial wastes are involved because many of these substances are resistant to biological or chemical degradation, and thus, are expected to persist in their original form for many years, perhaps even for centuries (Fatta, *et al*., 1999).

Groundwater from the quaternary aquifer is suitable for the use as a source of drinking water and for industrial uses. However, development of the contaminated sources in the study area is threatening the quality of the groundwater.

Contamination of groundwater can take place if the waste disposal site containing above substances gets leached and percolates into the groundwater table. Hence, no adverse impact on groundwater quality is anticipated in the present project. Even in the very long term (on a timescale of several 100 years), when these sources are continued, the potential impacts on groundwater quality are predicted to be slight.

The geophysical investigation revealed that the resistivity value of the study area near the dumpsite is relatively low about 3.0-4.0 Ω.m in VES points 2 and 3 compared to those of the uncontaminated areas outside the disposal site as we mentioned it. The electrical resistivity anomaly near the dumping site was related to septic tank discharges plumes which appear to have seeped at depth as far as 1.5 m below the surface.

The soil at the study area was found to be incapable of preventing the migration of contaminants, vertically and/or horizontally from the source point. Hence, this illustrates that the septic tank discharge valley has been polluting the soil as well as increasing its vulnerability not only to the soil and groundwater but also capable to have an effect on the fauna and flora.

The short pathway needed for these contaminants before reaching groundwater was enhanced by periodic water table fluctuations and infiltrating water during the rainy season. These metals accumulate near the soil surface and decrease with depth due to adsorption to soil particles. Adsorption occurs on surfaces of clay minerals, hydrous oxides or iron and aluminum, and organic matter (GWMAP, 1999). Furthermore, the nature of geology has important role to infiltrate the pollutants through it, as the geological composition of the study area is of clastic materials which have higher effect to infiltrate. This with time may reach to the groundwater and can contaminate it.

According to Shyler, *et al*. (2009), important soil characteristics that may affect the behavior of contaminants include soil mineralogy and clay content (soil texture); pH of the soil; amount of organic matter in the soil; moisture levels; temperature; and presence of other chemicals.

Septic waste discharged to coarse-textured soils proceeds vertically through the unsaturated zone and into groundwater (Fig. 16). Once in groundwater, a septic plume develops and moves with groundwater flow. Approximate times for septic effluent to pass through the unsaturated zone to groundwater range from a few hours to 50 days, depending on the volume of effluent and the distance to groundwater (Robertson, *et al*., 1991; Robertson, 1994 and Robertson and Cherry, 1995).

Nitrate is the primary chemical of concern in most septic plumes. Nitrate plumes slowly attenuate as a result of dilution from recharge water and dispersion within the aquifer. Nitrate concentrations can exceed drinking water criteria at distances of 100 m or more from the drain field (GWMAP, 1999).

Fig. 16 (a) Convoy of waste loading tankers heading toward the site, (b) sewage is discharged at one point, and (c) developing little stream as consequence to continued discharge

Factors that may affect an aquifer's susceptibility to nitrates and the concentration of nitrates in groundwater include land-use, climate, topography, groundwater flow, infiltration rates, subsurface biogeochemical conditions, bedrock types, and soil characteristics (Lindsey, *et al*., 1997; Nolan and Hitt, 2003).

XI. Conclusions and recommendations

Based on sample analysis and the interpretation of the resistivity data both qualitatively and quantitatively, seven types of curve types were obtained, and geoelectrical sections along three traverses conclude the following points:

1. The results of water sample analysis at three different locations show that they are within the acceptable limits according to the WHO (2003). All water analyzed samples are suitable for drinking and irrigation uses.
2. The results of soil sample analysis at three different locations at far distances away from the dumpsite show that they are clay loam types with pH of strongly alkaline with EC of 8.0- 13.0 m/cm.
3. In general, resistivity values indicate a decreasing trend with depth due to an increase in the fine sediments with some lateral changes.
4. The resulting geoelectric models are used to produce three geoelectric sections: Traverses A-A¯, B-B¯, and C-C¯. Each section has its characteristics of true resistivity, depth, and its lithology can be interpreted in detail, the following zones are outlined:
   - (Z1): A thin surface layer occurs in all traverses represented by topsoil with resistivity ranging from 28-421 Ω.m. These variations in resistivity value occur due to various types of materials, fine- and medium-grained material of sand and gravel. The thickness varies from 0.5 to 6.0 m.
   - (Z2): This zone has resistivity ranging from 3.0 to 40.0 Ω.m and composed of fine-grained sediments such as sand, silt, and clay with a thickness ranging from 1 to 18 m in traverses A-A¯ and B-B¯, whereas in the traverse C-C¯, the resistivity ranges from 27.0 to 99 Ω.m and the thickness ranges between 8.0 and 33.0 m. This layer is composed of a mixture of gravel, sand, silt, and clay.
   - (Z3): This zone has a resistivity ranging from 20.0 to 322.0 Ω.m and a thickness ranging from 6.0 to 58.0 m. This horizon is composed of a mixture of gravel, sand, silt, and clay. Within this horizon, the lenses or lateral changes occur with the resistivity ranges from 20.0 to 40.0 Ω.m, and the thickness ranges between 7.0 and 49.0 m) This horizon is composed of sand, silt, and clay.
   - (Z4): This zone has resistivity ranging from 11.0 to 50.0 Ω.m and a thickness ranging from 41.0 to 101.0 m. It consists of sand, silt, and clay, which represents an aquifer for groundwater in traverse C-C¯.
   - (Z5): This zone has a resistivity value ranging from 10.0 to 44.0 Ω.m and composed of silt and clay, in traverse B-B¯, the lens occurs which is composed of a mixture of gravel, sand, silt, and clay and has resistivity (61.0 Ω.m). Furthermore, the traverse C- C¯ is composed of silt and clay with lateral variation to sand and silt with resistivity ranges from 34.0 to 47.0 Ω.m. The thickness of this layer is not defined since it is the last layer.
5. The average depth from the surface to the top of the aquifer is about 80 m.
6. The septic tank discharges valley has been polluting the soil. While no adverse impact on groundwater quality is anticipated in the present project.
7. From the results of geoelectrical sections, the contaminated area occurred and revealed very low resistivity compared with surrounding area.
8. It iss recommended that the UNESCO program for solid waste management protocol should be enacted to ensure groundwater integrity in the urban parts of the region.

References

Adli, Z.H., Musa, M.H. and Arifin, M.N.K., 2010. Electrical resistivity of subsurface: Field and laboratory assessment. World Academy of Science, Engineering and Technology, 69, pp.805-808.

Al-Agidi, W.K., 1989. Pedology-soil survey and classification. *Ministry of Higher Education and Science Research, College of Agriculture, Soil Department.* Baghdad University, Mosul University Press, Arabic.

Al-Ansari, N.A., Hedeff, I.E. and Salim, Y.N., 1981. Water resources in Iraq. Journal of the Geological Society of Iraq, 14(1), pp.35-42.

Al-Naqib, K.M., 1959. Geology of the Southern Area of Kirkuk Liwa. Iraq, Iraqi Pet. Com. Ltd., pp.50

Arshad, M., Cheema, J.M. and Ahmed, S., 2007. Determination of lithology and groundwater quality using electrical resistivity survey. *International of Agriculture and Biology*, 9(1), pp.143-146.

Badmus, B.S., Ozebo, V.C., Idowu, O.A., Ganiyu, S.A., Olurin, O.T. and Atayese, A.O., 2014. Assessment of microbial contamination of groundwater near solid waste dumpsites in basement complex formation, using total plate count method. Nature and Science, 12(9), pp. 113-118.

Bernard, J., 2003. Short Notes on the Depth of Investigation of Electrical Methods. Available from: http://www.iris-instruments.com/Pdf_file/Resistivity_Imaging/methods_depth_investigation.pdf.

Buday, T., 1980. The regional geology of Iraq. *Stratigraphy and Paleogeography.* Vol. 1. Publications of GEOSURV, Baghdad, p445.

Chuangcham, U., Wirojanagud, W., Charusiri, P., Milne-Home, W. and Lertsirivorakul, R., 2008. Assessment of heavy metals from landfill leachate contaminated to soil: A case study of Kham Bon landfill, Khon Kaen province, NE Thailand. Journal of Applied Sciences, 8(8), pp.1383-1394.

Compbell, D.L. and Horton, R.J., 2000. *Graph and Tables Used to Describe Electrical Measurement of Samples of Unconsolidated Material.* USGS Petrophysical Laboratory-Denver, Open-File Report, Denver, p.16.

Dizayee, R., 2014. *Groundwater Degradation and Sustainability of the Erbil Basin, Erbil, Kurdistan Region, Iraq.* College of Science and Engineering, Texas Christian University, Fort Worth, Texas, p.84.

Edwards, L.S., 1977. A modified pseudo section for resistivity and IP. Geophysics, 42(5), pp.1020-1036.

Evanston., 1979. Earth Resistivity Manual. Evanston, Soil Test, INC. pp.52.

Fatta, D., Papadopoulos, A. and Loizidou, M., 1999. A study on the landfill leachate and its impact on the groundwater quality of the greater area. Environmental Geochemistry and Health, 21, pp.175-190.

Geoscan-M Ltd., 2001. *IPI2win Program, IPI- Res2, IPI- Res3 Users Guide. V. 2.1*. Moscow State University, Moscow, p.25.

Ghaib, F.A. and Aziz, B.K., 2002. A combination of electrical resistivity and gravity measurements for groundwater prospection in parts of Erbil city. Journal of Duhok University, 6(1), pp.105-111.

Ghaib, F.A., 2003. *Geophysical Survey for Groundwater in Some Selected Basins of Erbil Governorate. International Report*. FAO representation in Iraq, Erbil Sub-Office, p.69.

Gulmez, P., 1999. Predictive Tools in Environmental Impact Assessment of Solid Waste Projects. p.21.

GWMAP, Ground Water Monitoring and Assessment Program., 1999. *Effects of Septic Systems on Groundwater Quality.* Published by Minnesota Pollution Control Agency, Baxter, Minnesota, p.37.

Habib, H.R., Al-Saigh, N.H. and Hassan, Z.M., 1990. *Geochemistry of Under Groundwater in Erbil City, Iraq. Mosul University*, Mosul, Iraq, pp.173-188.

Hassan, E.O., 1998. *Urban Hydrogeology of Erbil City Region, Unpublished Ph.D. Thesis*, University of Baghdad, Iraq.

Jassim, S.Z. and Goff, J.C., 2006. *Geology of Iraq*. Published by Dolin, Prague and Moravian Museum, Brno, p.341.

Jegede, S.I., Ujuanbi, O., Abdullahi, N.K. and Iserhien-Emekeme, R.E., 2012, Mapping and monitoring of leachate plume migration at an open waste disposal site using non-invasive methods. Research Journal of Environment and Earth Science, 4(1), pp.26-33.

Knodel, K., Lange, G. and Voigt, H.J., 2007. Environmental geology, handbook of field methods and case studies. *Hannover Federal Institute for Geosciences and Natural Resources*. Springer Books, Heidelberg, p.1357.

Lashkaripour, G.R. and Nakhaei, M., 2005. Geoelectrical investigation for the assessment of groundwater conditions: A case study. Annals of Geophysics, 48(6), pp.937-944.

Lindsey, B.D., Loper, C.A. and Hainley, R.A., 1997. *Nitrate in Ground Water and Stream Base Flow in the Lower Susquehanna River Basin, Pennsylvania and Maryland, United States Geological Survey, Water-Resources Investigations Report 97-4146*. Lemoyne, Pennsylvania.

Lowrie, W., 1997. *Fundamentals of Geophysics.* Cambridge University Press, Cambridge. p.354.

Majeed, R.A. and Ahmad, M.A., 2002. *Brief References on Hydrogeological Characters of Erbil Basin*. Unpublished Report, Erbil-Iraq.

Mirsal, I.A., 2008. *Soil Pollution, Origin, Monitoring and Remediation*. 2nd ed. Springer, New York.

Munsell Book of Color, 1975. Munsell Color Co., Inc., Baltimore, Maryland, U.S.A.

Nolan, B.T. and Hitt, K.J., 2003. *Nutrients in Shallow Ground Waters Beneath Relatively Undeveloped Areas in the Conterminous United States, U.S. Geological Survey*. Water-Resources Report 02-4289, Denver, Colorado.

Oghenekohwo, F.O., 2008. A comparision of resistivity and electromagnetics as geophysical techniques. Postgraduate Diploma, 48, p.27.

Raju, N.J., Shukla, U.K. and Ram, P., 2011. Hydrogeochemistry for the assessment of groundwater quality in Varanasi: A fast-urbanizing center in Uttar Pradesh, India. Environmental Monitoring and Assessment, 173(1-4), 279-300.

Reynolds, J.M., 2011. *An Introduction to Applied and Environmental Geophysics*. Wiley-Blackwell, Chichester, UK, p.698.

Robertson, W.D. 1994. Chemical fate and transport in a domestic septic system: Site description and attenuation of dichlorobenzene. Environmental Toxicology and Chemistry, 13, pp.183-191.

Robertson, W.D. and Cherry, J.A., 1995. *In situ* denitrification of septic-system nitrate using reactive porous media barriers: Field trials. Ground Water, 33, pp.99-111.

Robertson, W.D., Cherry, J.A. and Sudicky, E.A., 1991. Ground-water contamination from two small septic systems on sand aquifers. Ground Water, 29, pp.82-92.

Shyler, H., McBride, M. and Harrison, E., 2009. *Sources and Impacts of Contaminants in Soils*. Cornell Waste Management Institute, Cornell University, Ithaca, NY, p.6.

Singh, S., Raju, N.J. and Nazneen, S., 2015a. Environmental risk of heavy metal pollution and contamination sources using multivariate analysis in the soils of Varanasi environs, India. Environmental Monitoring and Assessment, p.187. DOI: 10.1007/s10661-015-4577-4.

Sissakian, V.K., 1997. *Geological Map of Iraq, Scale 1:250000.* 1st ed. GEOSURV, Baghdad, Iraq.

Stevanovic, Z. and Iurkiewicz, A., 2009. Groundwater management in Northern Iraq. Hydrogeology Journal, 17, pp.367-378.

Telford, W.M., Geldart, L.P. and Sheriff, R.F., 1990. *Applied Geophysics.* 2nd ed. Cambridge University Press, Cambridge, p.770.

Vladimir, S., Rodríguez, O.D., Mousatov, A., Hernández, D.F., Martínez, H., Ryjov, A., 2006. Estimation of soil petrophysical parameters from resistivity data: Application to oil-contaminated site characterization. Geofísica Internacional, 45(3), pp.179-193

World Health Organization, WHO, 2003. *Guide Line for Drinking Water Quality*. 3rd ed., Vol. 1. WHO, Geneva, Switzerland, p.540.

Zohdy, A.A.R., Eaton, G.P. and Mabey, D.R., 1984. *Applications of Surface Geophysics to Groundwater Investigations: Department of Interior US Geological Survey, Third Printing.* US Government Printing Office, Washington, p.116.